Chapter 4
MODELLING ENCAPSULATION TISSUE AROUND COCHLEAR IMPLANT ELECTRODES

1 INTRODUCTION

Cochlear implant subjects often experience changes in threshold current during the first few months after implantation. During one study Pfingst (1990) reported that in 88% of cases thresholds were highest during a period some time during the first month after implantation and then decreased by 8 to 37 dB during the following weeks. Eddington et al. (1988) and Miller, Morris and Pfingst (2000) also found threshold reduction over the first two to three months postsurgery. Pfingst (1990) suggested that threshold reduction results from either changes in conductivity between the electrodes and the neural elements or changes in the sensitivity of the neural elements themselves.

Fibrous scar tissue and new bone often grow around intracochlear electrode arrays in animals and humans (Leake et al., 1992; Linthicum et al., 1991; Webb et al., 1988; Zappia et al., 1991). Tissue reaction to implanted materials can vary from toxic reactions (where inflammation and infection occur as a result of degradation of the implant material and/or implant orientation or geometry), to vital reactions where the body detects the foreign object and incorporates it into the body by covering it in a vascularized fibrous scar tissue encapsulation (Nanas, 1988). Perfect biocompatibility does not exist in the true sense of the word (Bertoluzza et al., 1992) since tissue reactions always occur to a greater or lesser extent at the biomaterial-tissue interface. Vital tissue reaction to intracochlear electrode arrays is thus the

desired tissue response and also the most frequently observed response.

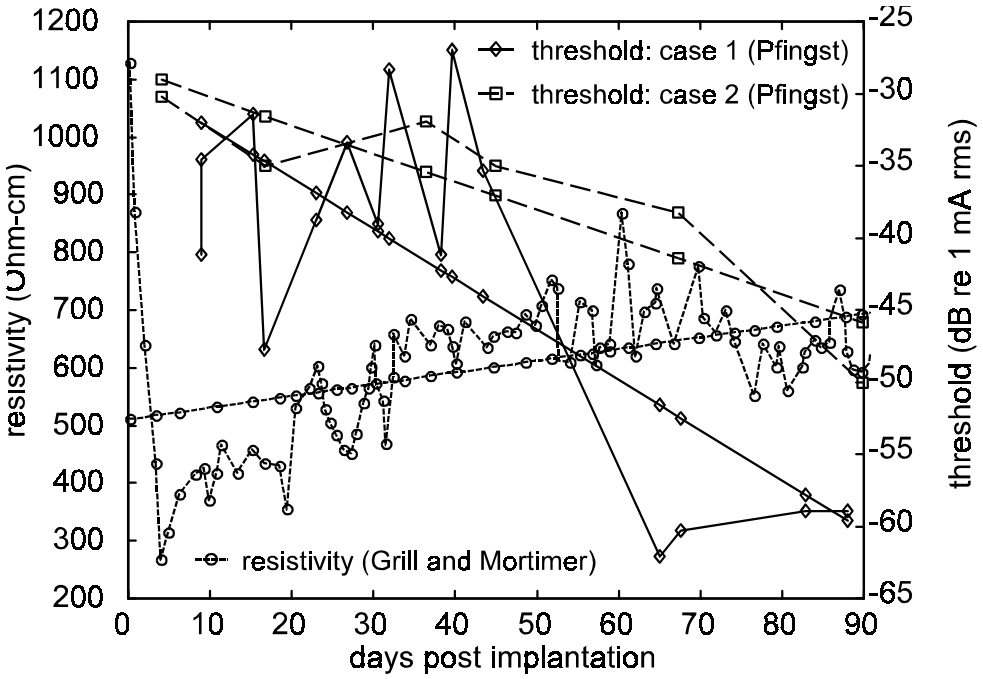

Figure 4.1. Impedance and threshold data as functions of time post-implantation after the data of Grill and Mortimer (1994) and Pfingst (1990). Impedance data are represented by resistivity in -cm while threshold currents are given in dB relative to 1 mA rms. Each set of data is represented by the original data (irregular lines) as well as a linear fit through the data (straight lines).

Tissue reactions to intracochlear electrodes range from very little fibrous tissue (Leake et al., 1992; Linthicum et al., 1991; Zappia et al., 1991), to a dense connective tissue cuff surrounded by loose, less-dense tissue (Zappia et al., 1991) around the implant inside the scala tympani. New bone sometimes envelops the electrode array in the scala tympani of the basal turn (Leake et al., 1992; Linthicum et al., 1991). Grill and Mortimer (1994) reported that the resistivity of encapsulation tissue is sufficient to alter the shape and magnitude of the electric field generated by chronically implanted electrodes. Clark et al. (1995) also suggested that bone and fibrous tissue formation in the cochlea could account for variations in patients' speech perception. Changes in the tissues surrounding cochlear implant electrodes can thus be

expected to affect the neural excitation patterns and therefore detection thresholds and dynamic ranges of electrical stimulation overall.

Pfingst (1990) found at most weak correlation between implant impedances and threshold changes during the first months after implantation, whereas De Sauvage et al. (1997) reported that compound action potential amplitudes and electrode impedance increased in correlation with each other. A comparison of the data of Grill and Mortimer (1994) and Pfingst (1990) suggests that while an increase in electrode impedance takes place, a decrease in threshold current occurs (Figure 4.1).

The objective of this chapter is to explain the effect of encapsulation tissue around cochlear implant electrodes on electrical potential distributions and auditory nerve excitation patterns during electrical stimulation.

2 MODEL AND METHODS

2.1 Combined finite element-nerve fibre model

The FE model of the first one-and-a-half turns of the electrically stimulated cochlea described in Chapter 2 was used to determine the effect of electrode encapsulation on the electrical potential distributions and thus neural excitation patterns during electrical stimulation. Two possible banded array locations were modelled: one at a medial location in the scala tympani (called banded medial or "BM") and one at a more lateral location in the scala tympani (called banded lateral or "BL"). Only one array existed during a specific simulation. An array was selected by changing the material properties of its elements to those of an insulator or a conductor, while changing the material properties of the other array to that of perylimph. Six electrode configurations were modelled corresponding to the first six configurations described in Table 3.1. The encapsulation tissue was modelled as a material layer with a resistivity of 627 -cm in direct contact with the electrode array. The resistivity of the encapsulation tissue is based on the measurements of Grill and Mortimer (1994) on

encapsulation tissue around electrodes implanted subcutaneously in cats. Grill and Mortimer (1994) reported an encapsulation tissue thickness of approximately 500 m. However, this fibrous tissue thickness was reported for subcutaneous implants and not intracochlear implants. In the FE model an encapsulation tissue thickness of 50 m was used based on observations of an average intracochlear fibrous tissue thickness around silastic electrode carriers of 48.5 m (Seldon et al., 1994) and to allow two electrodes surrounded by encapsulation tissue to fit within the scala tympani. Simulation results were generated for an electrode without encapsulation tissue (hereafter called "clean") and for an electrode surrounded by a 50 m layer of encapsulation tissue (hereafter called "encapsulated").

Electrical potential distributions generated by electrical stimulation with a 200 A dc current were calculated on a plane in the model (Chapter 2) containing the auditory nerve fibres.

2.2 Lumped-parameter model

A lumped-parameter (LP) model (Figure 4.2) of the implanted cochlea that incorporates the effect of fibrous tissue encapsulating an electrode array was created. The LP model illustrates the principle by which encapsulation tissue causes changes in the electrical potential and current at the target nerve fibres. The model is based on several LP models found in the literature (Kral et al., 1998; Strelioff, 1973; Suesserman & Spelman, 1993). Resistances included are for the perilymph in the scala tympani (R_p), the basilar membrane or bone separating the scala tympani from the scala media (R_b), the peripheral dendrites of the nerve fibres (R_n), an extracochlear current return pathway through the surrounding tissues (R_{e1} and R_{e2}) and radial and longitudinal components of the encapsulation tissue (R_r and R_l). The radial component of the encapsulation tissue represents the current pathway normal to the electrode surface and the longitudinal component represents the current pathway through the encapsulation tissue parallel to the electrode. Resistances of electrode contacts and the electrode carrier are not included since they are treated as perfect conductors and perfect insulators respectively. Each segment of the

model represents 200 m of the implanted cochlea. The model consists of 63 segments (12.6 mm) terminated with a 64th set of radial resistances equivalent to the radial resistances in the rest of the model.

Table 4.1. Description of circuit elements of LP model in Figure 4.2.

Circuit Element	Description	Value ( )	
		Clean	**Encapsulated**
R_p	Perilymph in scala tympani	700	700
R_b	Basilar membrane	8 000	8 000
R_n	Nerve fibres	3 000	3 000
R_{e1}	Extracochlear tissues	6 300	6 300
R_{e2}	Extracochlear current return pathway	6.3	6.3
R_r	Radial resistive component of encapsulation tissue	0	720
R_l	Longitudinal resistance component of encapsulation tissue	0	12 300

Resistance values are based on material properties used by Frijns et al. (1995), Grill and Mortimer (1994) and Kral et al. (1998). The resistivity of encapsulation tissue was approximated by application of the equation R = /A[1] in the radial and longitudinal directions and assuming that no current leaves the encapsulation tissue toward the electrode array except at the stimulating electrodes. Resistive values of

[1]R represents resistance, the resistivity of the encapsulation tissue, the length of the tissue in the direction of current flow and A the area of the annular region normal to the direction of current flow.

model components are given in Table 4.1.

2.3 Modelling of Auditory Nerve Excitation

Thresholds were determined with the generalized SEF auditory nerve fibre model (Frijns et al., 1995). Two types of nerve survival were modelled: one where the nerve fibres were intact and thus included the peripheral dendrites and another where the peripheral dendrites of the nerve fibres had degenerated. To simulate loss of peripheral dendrites, a truncated version of the generalized SEF model (Chapter 2) was used.

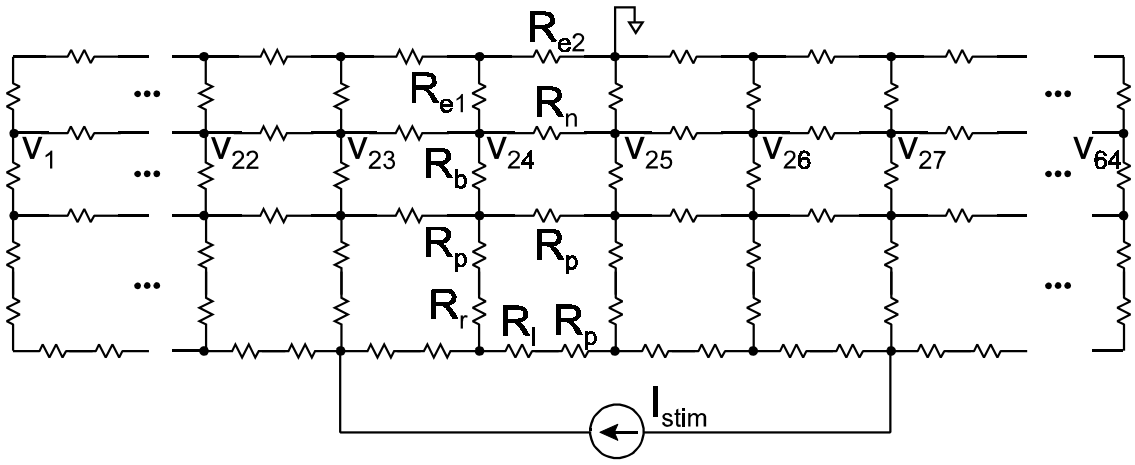

Figure 4.2. Schematic representation of LP model of intracochlear stimulation with radial and longitudinal resistances of encapsulation tissue included. Refer to Table 4.1 for component values.

The stimulus was a 200 s per phase charge balanced biphasic current pulse generated by scaling the electrical potentials predicted by the FE model. The threshold current for a nerve fibre was defined as the lowest current level that excited the nerve fibre during a single stimulation cycle. Nerve excitation was assumed when a propagating action potential occurred (Reilly et al., 1985).

3 RESULTS

3.1 Electrical potential distributions

The electrical potential amplitude and the spread of the electrical potential along the length of the basilar membrane are overestimated by the LP model. The slight differences in the prediction of the location of the maximum and minimum electrical potential amplitudes between the LP and FE models can be attributed to dimensional variations between the two models.

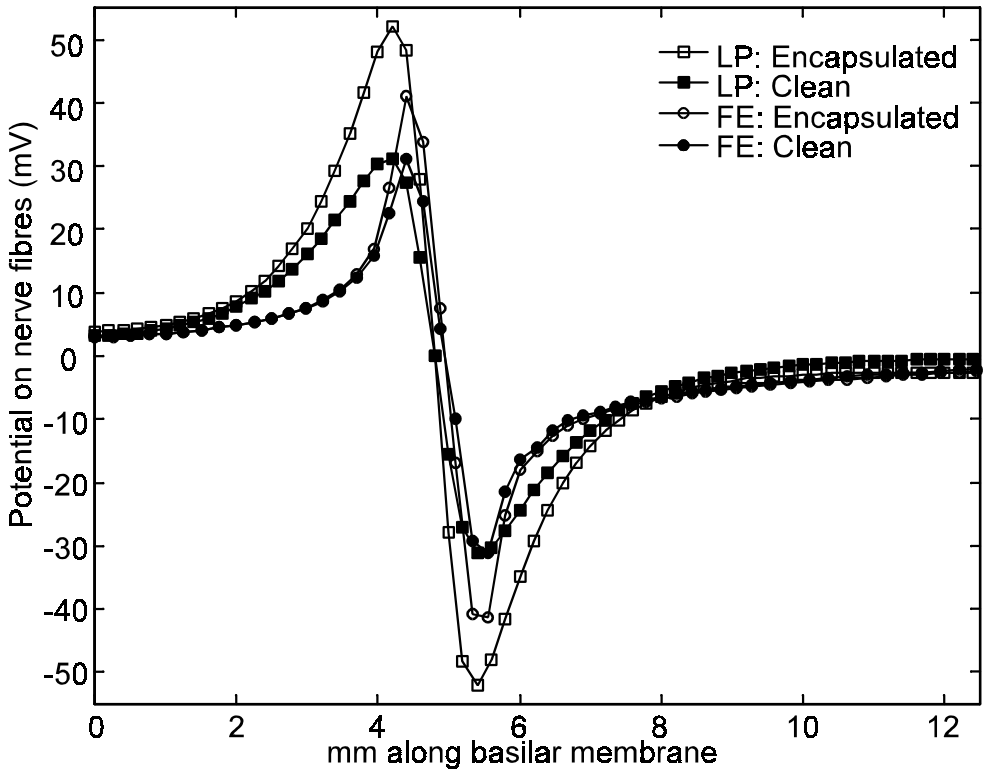

Figure 4.3. Comparison of electrical potential distributions along the basilar membrane predicted by the LP and FE models for BP electrode configuration.

Both models predict higher electrical potential amplitude deviations at the target nerve fibres in the presence of encapsulation tissue than in its absence. Figure 4.3 shows electrical potential distributions along the length of the basilar membrane calculated at the nerve fibres with the LP and FE models. At this location in the model, an increase of approximately 20 mV_{p-p} can be seen in the electrical potential

for the FE model and an increase of approximately 42 mV_{p-p} for the LP model. At the electrode contacts the FE model predicts an increase of approximately 90 mV_{p-p} while the LP model predicts an increase of 265 mV_{p-p} as a result of electrode encapsulation. If the radial resistive component of the encapsulation tissue in the LP model is increased, the potential at the target nerve fibres remains unchanged (Figure 4.3), but the potential at the electrode contacts increases substantially (to 478 mV_{p-p} if R_r is doubled).

3.2 Auditory nerve excitation

3.2.1 Minimum threshold current as a function of electrode encapsulation

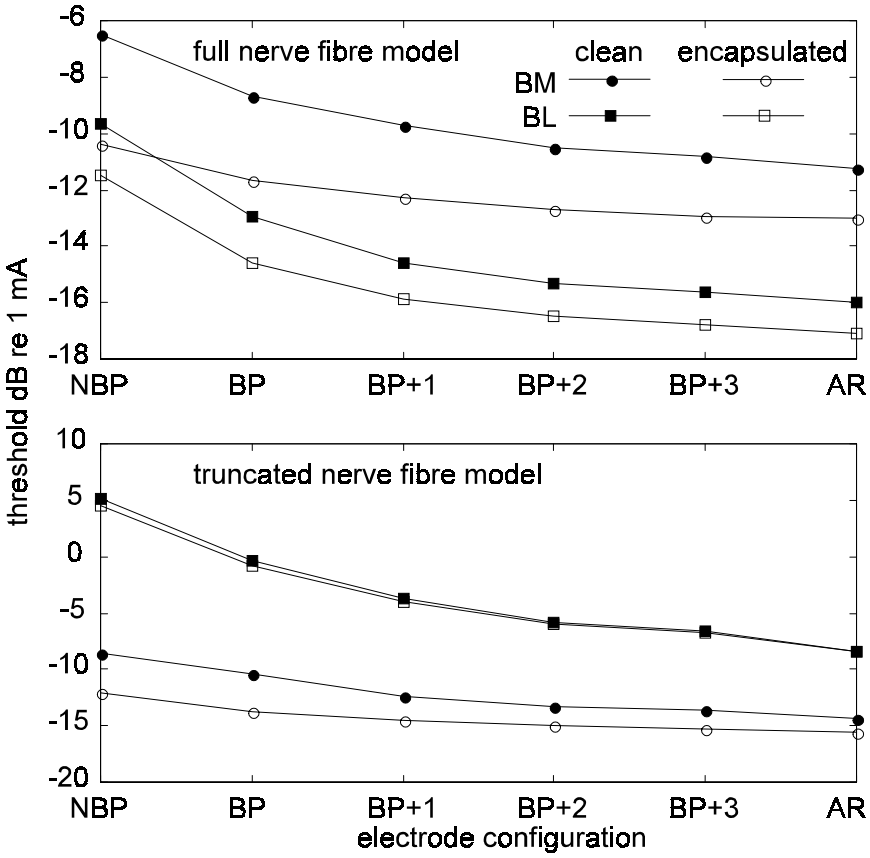

Figure 4.4. Threshold current as a function of electrode configuration in the presence and absence of electrode encapsulation for a full nerve model (upper graph) and a truncated nerve model (lower graph).

Figure 4.4 summarizes threshold currents determined with the combined FE-nerve model while Figure 4.5 shows the differences in threshold currents between clean and encapsulated electrodes. Threshold currents are generally reduced in the presence of encapsulation tissue. A maximum reduction in threshold current of 3.5 to 4 dB occurs for closely spaced (NBP) electrode configurations close to the modiolus (BM array). The smallest threshold current reduction is predicted for array locations far from the target nerve fibres using widely spaced (AR) electrode configurations, i.e., 0 to 1 dB for the BL array.

3.2.2 Spread of excitation

Spread of excitation was evaluated with electrical tuning curves (Figure 4.6) that show threshold current profiles for the nerve fibre array as a result of electrical stimulation. Electrical tuning curves for BP and AR1 electrode configurations for full (upper set of graphs) and truncated (lower set of graphs) nerve fibre models are shown.

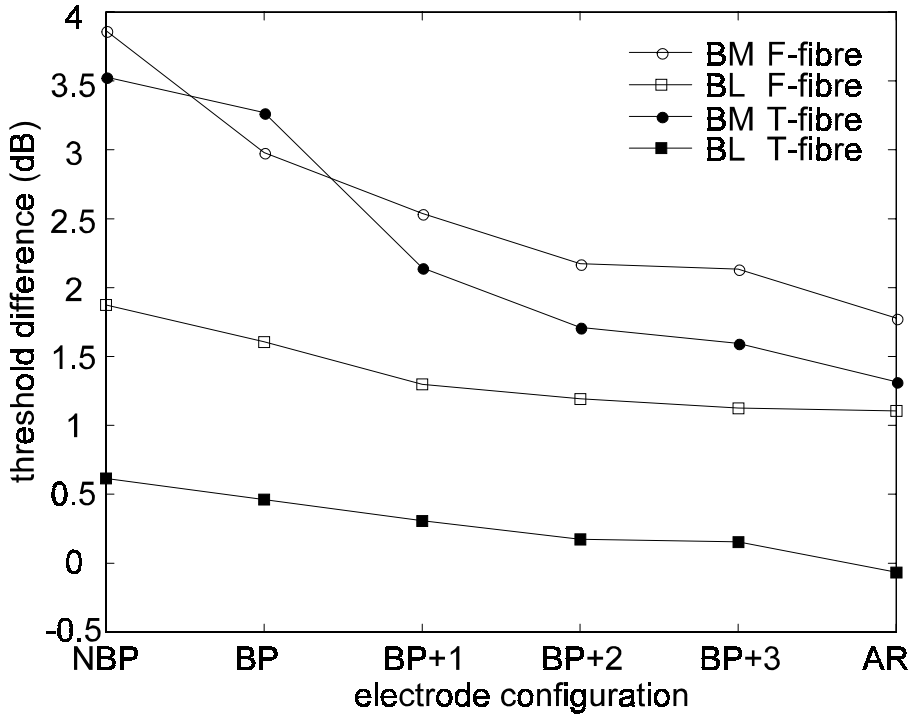

Figure 4.5. Threshold differences between clean and encapsulated electrode arrays as a function of electrode configuration.

Excitation patterns are different for clean electrodes and electrodes encapsulated with fibrous tissue. To evaluate this difference in excitation patterns, spread of excitation along the basilar membrane at 10 dB above threshold was plotted as a function of electrode separation (Figure 4.7). In general, the presence of encapsulation tissue around electrode arrays limits (narrows) the spread of excitation noticeably (up to 1 mm). The exception is where the array is located far from the target nerve fibres where virtually no difference in the spread of excitation occurs between clean and encapsulated arrays, e.g., the BL array for the truncated nerve model.

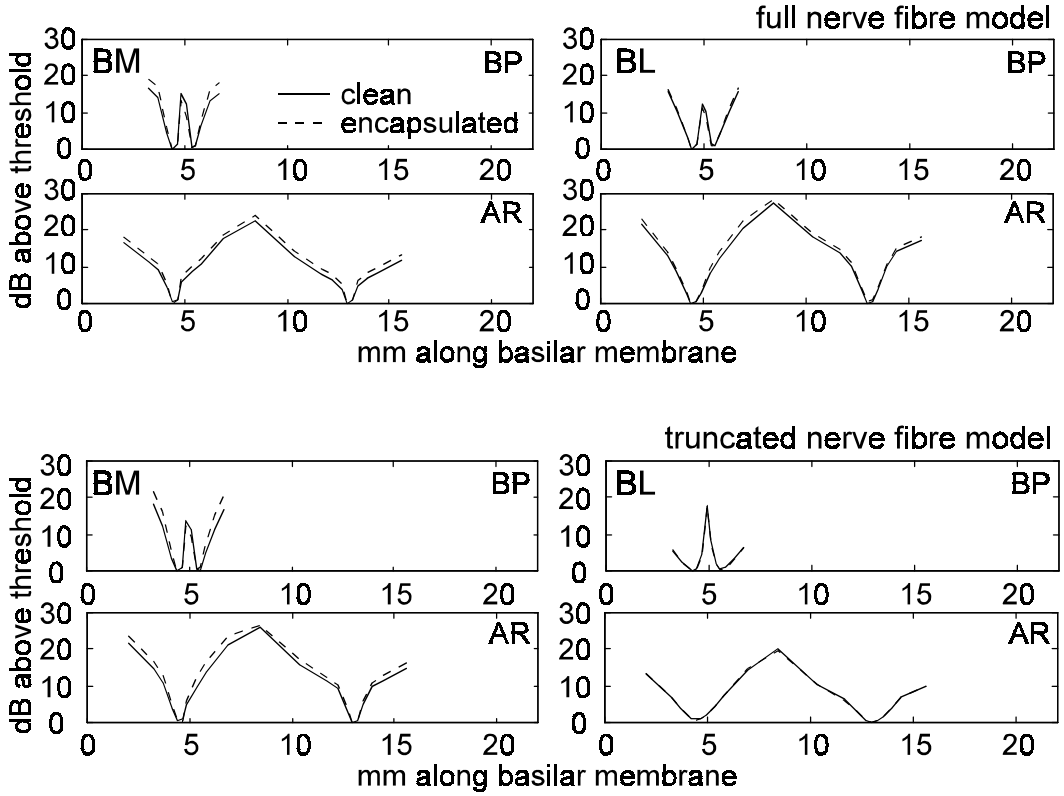

Figure 4.6. Electrical tuning curves for the P array for a full nerve fibre model (upper set of graphs) and a truncated nerve fibre model (lower set of graphs).

4 DISCUSSION

Both the FE and LP models predict an increase in the electrical potential amplitude at the target nerve fibres in the presence of encapsulation tissue. The mechanism responsible for the increase in electrical potential can be explained by the LP model.

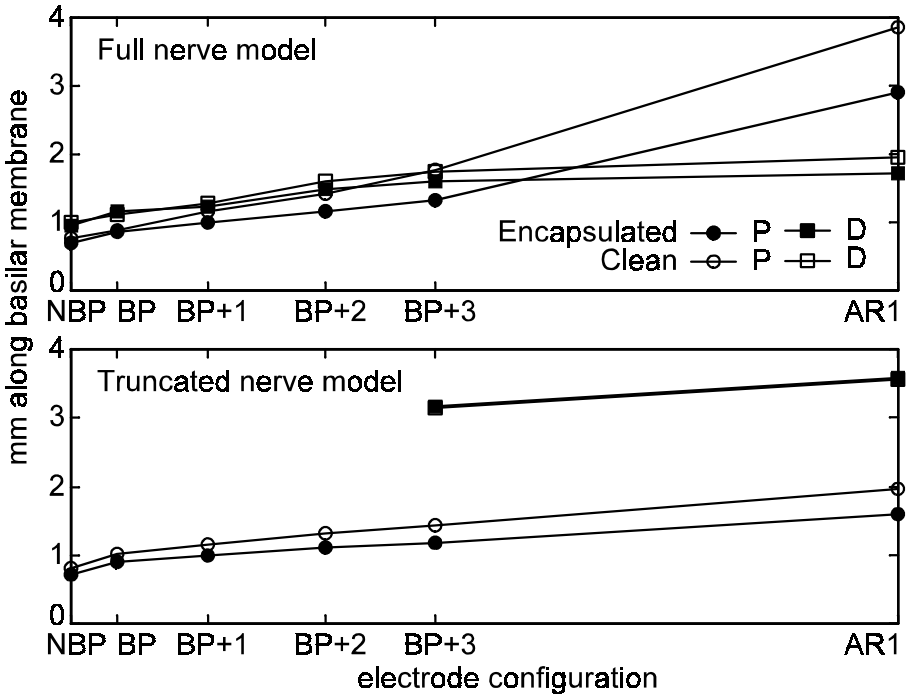

Figure 4.7. Spread of excitation along the length of the basilar membrane as a function of electrode separation at a stimulus intensity of 10 dB above threshold. The locations of electrode configurations on the abscissa have been scaled to represent their respective interelectrode spacings in the FE model. Spread of excitation has not been plotted for narrowly spaced electrode configurations for the BL array using the truncated nerve model (lower graph) since the spread of excitation exceeded the region over which thresholds were calculated.

The two resistances representing the encapsulation tissue in the LP model each has a specific effect. The longitudinal resistance R_l of the encapsulation tissue is responsible for the increase in electrical potential at the target nerve fibres, while the

radial resistance R_r is responsible for an increase in electrical potential at the electrode contacts. If R_r becomes very high, compliance problems may occur near the upper limits of dynamic range since the stimulator may not be able to drive the current into the increased load resistance. This might be especially true for narrowly spaced electrode pairs, e.g. the offset radial electrode pairs of the electrode of the Clarion implant (Kessler, 1999), where loudness growth problems frequently occur. The effect of R_l can be explained by observing that the network branch containing R_l carries a part of the current injected by the current source (I_{stim}) along the length of the model. If the resistance in this branch is increased, i.e., R_l increases, more current will be forced into the other parallel branches, causing the electrical potential across these branches to increase. Encapsulation tissue therefore increases the resistance of the current pathways close to the electrode carrier, thereby forcing the current through more remote pathways. Such remote pathways could include the nerve fibres, as is suggested by both the FE and LP models. The primary effect of R_l is thus to increase the electrical potential (and currents) that occur at the nerve fibres and consequently to lower the current levels at which nerve excitation will occur.

The effect of R_l can be seen in the decrease of minimum threshold currents in the presence of encapsulation tissue (Figures 4.4 and 4.5) and is a function of both array location and electrode separation. For array locations far from the target nerve fibres and widely spaced electrode configurations the effect of encapsulation tissue is limited by greater volumes of cochlear tissue between the electrodes and the target nerve fibres. One would therefore expect to see more pronounced threshold current reductions because of electrode encapsulation for implants with arrays close to the modiolus, e.g., the Clarion (Kessler, 1999) cochlear implant, than for implants with arrays far from the modiolus, e.g., the Nucleus (Clark, 1996) cochlear implant. Some evidence for this observation can be found in threshold current reductions over time reported by Pfingst (1990) (who used arrays that positioned electrode contacts in the region between the modiolus and the middle of the scala tympani) and Dorman et al. (1992) (for patients using the Ineraid cochlear implant), while unchanged EABR

thresholds over time were reported for Nucleus implant users (Brown et al., 1995) Threshold current reduction predicted by the combined FE-nerve model occurs at a maximum rate of 0.2 dB per day[2]. This is comparable to threshold current reductions of 0.2 to 1 dB per day reported by Pfingst (1990). More severe threshold reduction predictions as a result of electrode encapsulation can be modelled by increasing the thickness of the encapsulation tissue in the FE model. The weak correlation between implant impedance and threshold current changes observed by Pfingst (1990) could be because the relatively high electrode-body fluid interface impedance, i.e., 10 to 20 k (de Sauvage et al., 1997; Dorman et al., 1992), dominates resistance changes caused by encapsulation tissue in the neighbouring cochlear tissues. Brown et al. (1995) reported slight but significant reduction in EABR slope with time for subjects implanted with the Ineraid implant. EABR slope gives an indication of the increase or decrease in the number of excited nerve fibres. EABR slope can thus be interpreted as a measure of spread of excitation and dynamic range, i.e., a shallower EABR slope corresponds with a narrower region of excitation (a slow increase in the number of excited nerve fibres with increasing stimulation current) and a larger dynamic range (Frijns, de Snoo & Schoonhoven, 1995). Model results indicate that spread of excitation is reduced by the presence of encapsulation tissue (Figures 4.6 and 4.7). This suggests that dynamic range could be increased by the presence of encapsulation tissue. Similar to threshold current reduction, encapsulation of electrodes mainly influences spread of excitation for array locations close to the target nerve fibres.

Although reduction in spread of excitation as a result of electrode encapsulation appears to be small (less than 1 mm in most cases), it cannot be ignored. Since the neural resolution of the model is rough, i.e. each modelled nerve fibre represents approximately 224 real nerve fibres, noticeable but small reductions in spread of excitation amounts to at least 224 nerve fibres for which the threshold current of an

[2]Average threshold current reduction rate calculated over a period of 25 days using the reduction in threshold current as a result of electrode encapsulation and assuming that the encapsulation thickness reaches the modelled 50 m after 25 days.

electrode pair has changed.

Results presented in this chapter suggest that electrode encapsulation can alter the shape and magnitude of the electric fields produced by intracochlear electrode arrays. These changes are reflected in reduction in threshold currents and spread of excitation. Cochlear implant subjects also show improved speech recognition performance from one to nine months post implantation (Tye-Murray et al., 1992) which could indicate an increased sensitivity developed for electrical stimulation. Also, for array locations close to the modiolus an increase in sensitivity to electrical stimulation could be a result of the degeneration of the peripheral dendrites of the auditory nerve fibres (Chapter 3). The mechanism responsible for the decrease in threshold current could thus be a combination of electrode encapsulation, sensitization for electrical stimulation and in some cases degeneration of the peripheral dendrites of the auditory nerve fibres.

5 CONCLUSION

An LP model of the implanted cochlea was presented to explain the mechanism by which encapsulation tissue could induce changes in threshold currents. It was found that a longitudinal resistive component of encapsulation tissue around cochlear implant electrodes causes currents and thus electrical potentials at the target nerve fibres to increase, while a radial resistive component causes an increase in the electrical potential at the electrode contacts.

The effect of electrode encapsulation was described through changes in threshold currents and spread of excitation. A combined FE-auditory nerve fibre model was used to quantify this effect. The effect of electrode encapsulation on neural excitation is controlled by electrode separation and array location. Narrowly spaced electrode configurations and array locations close to the modiolus are most sensitive to the effects of electrode encapsulation. Electrode encapsulation could be beneficial

since its presence could (1) decrease thresholds with 0.5 to 4 dB according to model results and (2) limit spread of excitation with up to 1 mm for widely spaced medial arrays, and thus increase dynamic range. However, if the radial resistive component of the encapsulation tissue becomes very high, compliance problems may arise at the upper end of the dynamic range of an electrode pair.